SRISTI - *The* NAL method for the design and analysis of natural laminar flow (NLP) airfoils

K.R. Srilatha, G.S. Dwarakanath, and P.Ramamoorthy

Computational and Theoretical Fluid Dynamics Division
National Aerospace Laboratories, Bangalore 560 017, INDIA

Abstract: A software package (called SRJSTI) for the design and analysis of NLF airfoils is described. As an illustration, an NLF airfoil for NAL's Light Transport Aircraft has been designed using this package. Its aerodynamic characteristics have been extensively compared with GAW-2 airfoil and also with wind tunnel experiments.

1. Introduction

There is a constant endeavour to seek energy efficient technologies for general aviation, and the design of Natural Laminar Flow (NLF) airfoils provides one. In this technology the flow is controlled to laminar on its own so as to reduce the profile drag. The availability of advanced materials for fabricating clean control surfaces without the usual surface roughness and the availabilty of good computational methods to custom-design any aerodynamic shape have paced this technology. NLF airfoils find applications in Remotely Piloted Vehicles (RPV), gliders, wind turbines, sports aircraft and other general aviation aircraft.

2. A brief survey of NLF airfoil design and development

Even before NLF airfoils were realised in practice in the 1990's, there were continuous and concerted efforts in the development of low drag airfoils at established aeronautical institutes in Europe and the U.S.A. Until 1920, airfoil development was mostly empirical in nature. By 1940 both NACA and Göttingen in Germany had developed airfoils using wind tunnel testing and potential flow theories. Even though some success was achieved in getting good stalling characteristics, premature transition to turbulence plagued the designers. In the 1950's NASA was able to achieve extensive laminar flow on airfoils and thereby cut down the drag by about 50%. The design of these airfoils (denoted by 6 digits) included the viscous effects through boundary layer theory unlike the earlier 4- and 5-digit series. In the 1960's there was a surge of interest in developing supercritical airfoils at transonic speeds and some interesting airfoils were developed by Whitcomb (1974) and others. In the 1970's, when the oil crisis hit the scene there were renewed efforts to obtain low speed versions of these supercritical airfoils; GAW-1 and GAW-2 airfoils were the outcome of these efforts. Since the 1980's there have been systematic efforts to design and develop tailormade NLF airfoils using advanced techniques of Computational Fluid Dynamics (CFD). NAL has also made contributions in this direction.

3. The design methodology - basic issues

In the last six decades the task of designing an airfoil to meet given specifications remained a difficult nut to crack even for the best brains. The first attempt was to an airfoil for a given upper surface surface distribution without addressing oneself to design issues which demanded such pressure distributions. Some of the work at R carried out by Germain (1945), Goldstein (1948), Lighthill (1945), Thwaites (1945a) and others was of this nature. Goldstein even succeeded in obtaining exact solutions the airfoil contour for a class of upper surface pressure distributions.

The major flaw in this approach was the neglect of the issues related to the bound layer, such as transition and separation. These play a dominant role in the design such airfoils. It is only in the last two decades that Wortmann (1973), Liebeck (1973) McMasters *et al.* (1979) and Miley (1974) started designing laminar airfoils with primary emphasis on boundary-layer management. While these approaches are steps the right direction, obtaining a suitable airfoil for supporting real viscous flows still rema an art rather than a science and no universal foolproof method seems to exist. Hence th is a need for such a method. The NAL method aims to meet these requirements by a t pronged approach of inviscid and viscous analysis: firstly we obtain an airfoil contc for supporting a nonviscous velocity distribution appropriate to a low drag airfoil, a secondly, test this airfoil for realistic performance using a viscous code. Figure 1 brir out the intricate connections between the airfoil shape, the inviscid pressures and t boundary-layer interaction.

For the inviscid design we use the classical solution of Goldstein (1948) to obtain symmetrical airfoil that supports a prescribed velocity distribution appropriate to low dr airfoils. The velocity distribution is conceived as a three-tier distribution (Fig. 2) and characterised by a few parameters. These parameters are: the initial acceleration (a), t magnitude and position of the maximum velocity $(6, x_1)$, the extent of the transition ran (c, x_2) and the concave recovery (γ, d) in the turbulent boundary layer region. The parameters can be tuned to obtain realistic symmetrical airfoils. Next, an appropria NASA camber line giving the desired lift arid pitching moment and maintaining a consta load from the leading edge to the trailing edge is superposed on this symmetrical airfo Finally the viscous performance of this airfoil is obtained. For this, an excellent, robu viscous code issued. This design procedure is repeated if the target performance is m achieved. Figure 3 gives the flow chart of the design process. The robustness of the NCS code (Ramamoorthy *et al.* 1987) is illustrated in Fig. 4 where the theoretical predictio are compared with experimental values for the NACA 64_3—418 airfoil. What in the effe the NAL method (Srilatha *et al* 1990, Srilatha and Ramamoorthy 1990) does is th it provides a mathematical model of the airfoil that is supposed to provide a low dra performance. It then tests this model in a numerical wind tunnel in the form of the NCS code. It repeats this procedure till the target performance is obtained.

4. The NAL method - an illustrative example

The NAL method is best illustrated for the design of an NLF airfoil of 13% thicknes for the design condition $M = 0.6$ $R_N = 10^6$ and $C_L = 0.4$. Firstly a surface pressur distribution characterised by

a	b	C	d	γ	x_1	$X2$	y_{max}
0.115	0.172	0.167	-0.194	-1.21	0.544	0.698	0.068

is chosen. As seen from Fig. 2 the velocity distribution is given by

$$\frac{v}{v_0} \approx 1 + g_s(\theta), \quad x = \sin^2(\frac{\theta}{2})$$

where

$$g_s(\theta) = \begin{cases} a_0 + a_1 \cos\theta & 0 \le \theta \le \theta_1 \\ 60 + b_1 \cos\theta & \theta_1 < 0 < \theta_2 \\ c_0 + c_1 \cos 6 + c_2 \cos 20 & \theta_2 < 0 < \text{fl"} \end{cases} \tag{1}$$

The continuity of $g_s(\theta)$ at θ_1, θ_2 results in

$$\begin{aligned} a_0 &= \frac{(b - a\cos\theta_2)}{(1 - \cos\theta_1)} \\ a_1 &= \frac{(a-b)}{2x_1} \\ \omega_0 &= \frac{(c\cos\theta_1 - 6\cos\theta_2)}{(\cos\theta_1 - \cos\theta_2)} \\ b_1 &= \frac{(b-c)}{2(x_2 - x_1)} \\ c_0 &= \frac{2c(1 + 4\cos\theta_2) + \cos\theta_2(\gamma + 8d\cos\theta_2) - \cos 2\theta_2(-\gamma + 2d)}{4(1 + \cos\theta_2)^2} \\ c_1 &= -\frac{(7 + 8\cos\theta_2) - 8c\cos\theta_2 - 7\cos 202}{4(1 + \cos\theta_2)^2} \\ c_2 &= -\frac{(\gamma - 2d) + 7\cos 02 + 2c}{4(1 + \cos\theta_2)^2} \end{aligned} \tag{2}$$

Now by Glauert's theory, the surface slope, $y_s'(\theta)$ and the perturbation velocity, $g_s(\theta)$ are related by the following expressions:

$$g_s(\theta) = \frac{1}{\pi} \int_0^\pi \frac{y'(\alpha)\sin\alpha d\alpha}{(\cos\alpha - \cos\theta)} \tag{3a}$$

$$y_s(\theta) = \frac{\sin\theta}{2\pi} P \int_0^\pi \frac{G(\theta) d\alpha}{(\cos\theta - \cos a)} \tag{3b}$$

where

$$(7(0) = \int_0^\theta g_s(\alpha)\sin\alpha \, d\alpha$$

and P denotes the Cauchy's principal value of the integral. Substituting Eq. (1) into Eq. (3b) and integrating, one gets the surface coordinates as

$$2\pi y_s(\theta) = \chi_1 \log\left\{\frac{\sin\frac{(\theta_1 - \theta)}{2}}{\sin\frac{(\theta_1 + \theta)}{2}}\right\} + \chi_2 \left\{\frac{\sin\frac{(\theta - \theta_2)}{2}}{\sin\frac{(\theta + \theta_2)}{2}}\right\} + \chi_3 \sin\theta + \chi_4 \sin 2\theta + \chi_5 \sin 3\theta$$

where

$$\chi_1 = \frac{1}{12}\{3(a_1 - b_1)(\cos 2\theta - \cos 2\theta_1) - 6(2a_0 - 2b_0)(\cos\theta - \cos\theta_1)\}$$

$$\chi_2 = -\frac{1}{12}\{2c_2(\cos 30 - \cos 3\theta_2) + 3(b_1 - c_1)(\cos 2\theta - \cos 2\theta_2) + 6(2b_1 - 2c_0 + c_2)(\cos 0 - \cos\theta_2)\}$$

$$\chi_3 = \frac{1}{6}\{3(2c_0 - c_2)\pi + 6(a_0 - b_0)\theta + 3(2b_0 - 2c_0 + c_2)\theta_2 + 3(a_1 - b_1) + 3(b_1 - c_1)\sin(9 - c_2 \sin 2\theta_2\}$$

$$X4 = \frac{1}{12}\{3c_1\pi + 3(a_1 - b_1)\theta_1 + 3(b_1 - c_1)\theta_2 - 4c_2 \sin\theta_2\}$$

$$Xs = \frac{1}{6}c_2(\pi - \theta_2)$$

Now the velocity at any lift coefficient C_L is given by Goldstein's second approximat a as

$$\frac{v}{v_0} \approx \frac{1 + \frac{1}{2}c_0^2}{(\psi_s^2 + \sin^2\theta)^{1/2}}\left[(1 + g_s(\theta))\sin\theta \pm C_L\left\{\frac{1}{2\pi} + \frac{\cos\theta}{a_0}\right\}\right]$$

where

$$\psi_s = \frac{2y_s}{\sin\theta}, \quad c_0 = \frac{1}{2\pi}\int_0^{2\pi}\psi(\theta)\,d\theta, \quad a_0 = \frac{dC_L}{d\alpha}$$

Figure 5 shows the pressure distribution on this symmetrical airfoil as obtained Goldstein's theory. On this symmetrical airfoil a NASA camberline of lift c_{L_i} = 0.27 a I constant load from leading to trailing edge was superimposed. In this case the airf I coordinates are given by

$$y_u = y_c + y_s\cos a$$
$$y_l = y_c - y_s\cos a$$
$$x_u = x - y_s\sin a$$
$$x_l = x + y_s\sin\alpha$$

where

$$y_c = \frac{c_{L_i}}{2\pi(a+1)}\left\{\frac{1}{2(1-a)}\left[(a-x)^2\log|a-x| - \frac{1}{2}(a-x)^2 - (1-x)^2\log|1-x| + \frac{1}{2}(1-x)^2 - x\log x + g - hx\right\}\right.$$

and

$$g = -\frac{1}{1-a}\left[a^2\left(\frac{1}{2}\log a - \frac{1}{4}\right) + \frac{1}{4}\right]$$

$$h = \frac{1}{1-a}\left[\frac{1}{2}(1-a)^2\log(1-a) - \frac{1}{4}(1-a)^2\right] + g$$

Again, the velocity distribution by Goldstein's third approximation is given by

$$\frac{v}{v_0} \approx AF\sin(\theta \pm e \mp 0) \pm BF\cos(\theta \pm \epsilon \mp \beta) \pm CF$$

where

$$A = (1 - \frac{C_L^2}{c_0^2})^{\frac{1}{2}} \quad B = \frac{C_L}{c_0} \quad C = \frac{C_L e^{c_0}}{2\pi}, \quad \beta = \epsilon(\pi)$$

and

$$\epsilon(\theta) = -\frac{1}{2\pi} P \int_0^{2\pi} \psi(\alpha) \cot \frac{\quad}{2} \, , \quad = \frac{\quad + \epsilon')}{(\psi^2 + \sin^2\theta)^{\frac{1}{2}}}, \quad \psi = \frac{2y}{\sin\theta}$$

Figure 6 illustrates the pressure distribution on this airfoil. This pressure distribution clearly shows that there is a good accelerated flow on both the upper and lower surfaces at the design C_L. This airfoil designated as NAL-NLF-136 was tested by the NCSU code for performance and compared with that of GAW-2. Figure *1* gives the comparison of pressure distribution for these two airfoils at the design $C_L = 0.4$. Figures 8-10 illustrate the lift, drag and pitching moment coefficients for NAL-NLF-136 and GAW-2 airfoils. One can see the better performance of NAL airfoil in terms of larger L/D in the operating C_L range.

NAL has utilised this design method to design two other NLF airfoils designated as NAL-NLF-208 and NAL-NLF-120 for NALLA and for an RPV respectively (Srilatha *et al.* 1990, Srilatha and Ramamoorthy 1990). Figure 11 gives the contours of these airfoils.

5. Wind tunnel and flight testing of the NAL-NLF-136 airfoil

Wind tunnel tests were conducted at the NAL $V \times 1'$ tunnel to study the off-design performance of the NAL-NLF-136 airfoil whose design procedure was explained above. A mild steel model of chord 6" was tested at $M = 0.52$ and $R_N = 2.6 \times 10^6$. Figure 12 shows the comparison between theory and experiment. One can see that for the off-design condition the theory and the experiments show an excellent correlation. Efforts are also under way for testing the NALLA NAL-NLF-208 airfoil using gliders. This airfoil was originally designed for the NAL Light Aircraft (NALLA).

8. Concluding remarks and future directions

Using the computational and wind tunnel resources at NAL it has been possible to design and develop NLF airfoils for general aviation applications. Efforts for testing these airfoils in a low turbulence tunnel are under consideration. Design of finite wings (with NLF wing sections) using a full-potential code and 3-D boundary layer calculations are under active exploration.

References

Germain, P. (1945), "The computaion of certain functions occuring in profile theory," ARC Rep. No. 8692.

Goldstein, S. (1948), "Low drag and suction airfoils," *J. Aero. Sci.*, 15(4).

Liebeck, R.H. (1973), "A class of airfoils designed for high lift in incompressible flow," *J. Aircraft*, 10(10).

Lighthill, M.J. (1945), "A new method of two dimensional aerodynamics design," R and M No. 2112, ARC.

McMasters, J.H. and Henderson, M.L. (1979), "Low speed single element airfoil analysis - Part I," NASA CP-2085.

Miley, S.J. (1974), "On the design of airfoils for low Reynolds numbers," *Proc. 2nd Int. Conf. on Tech. and Sci. of Low Speed and Motorless Flight*, MIT, Cambridge, Mass.

Ramamoorthy, P. and Dhanalakshmi, K. (1987), "NCSU Code: Validation and extension on NAL's UNIVAC 1100/60 system, NAL PD FM-8760.

Srilatha, K.R., Dwarakanath, G.S., and Ramamoorthy, P. (1990), "Design of a nat ral laminar flow airfoil for a light aircraft," *J. Aircraft,* **27**(11).

Srilatha, K.R. and Ramamoorthy, P. (1990), "Design of a natural laminar flow airfoi or an unmanned aircraft," NAL PD CF-9004.

Thwaites, B. (1945a), "A method of airfoil design - Part I," R and M No. 2166, ARC

Thwaites, B. (1945b), "A method of airfoil design - Part II," R and M No. 2167, AR(

Whitcomb, R.T. (1974),"A review of NASA supercritical airfoils," ICAS Paper 74-10.

Wortmann, F.X. (1973), "A critical review of the physical aspects of airfoil design at w Mach numbers," NASA CR-2315.

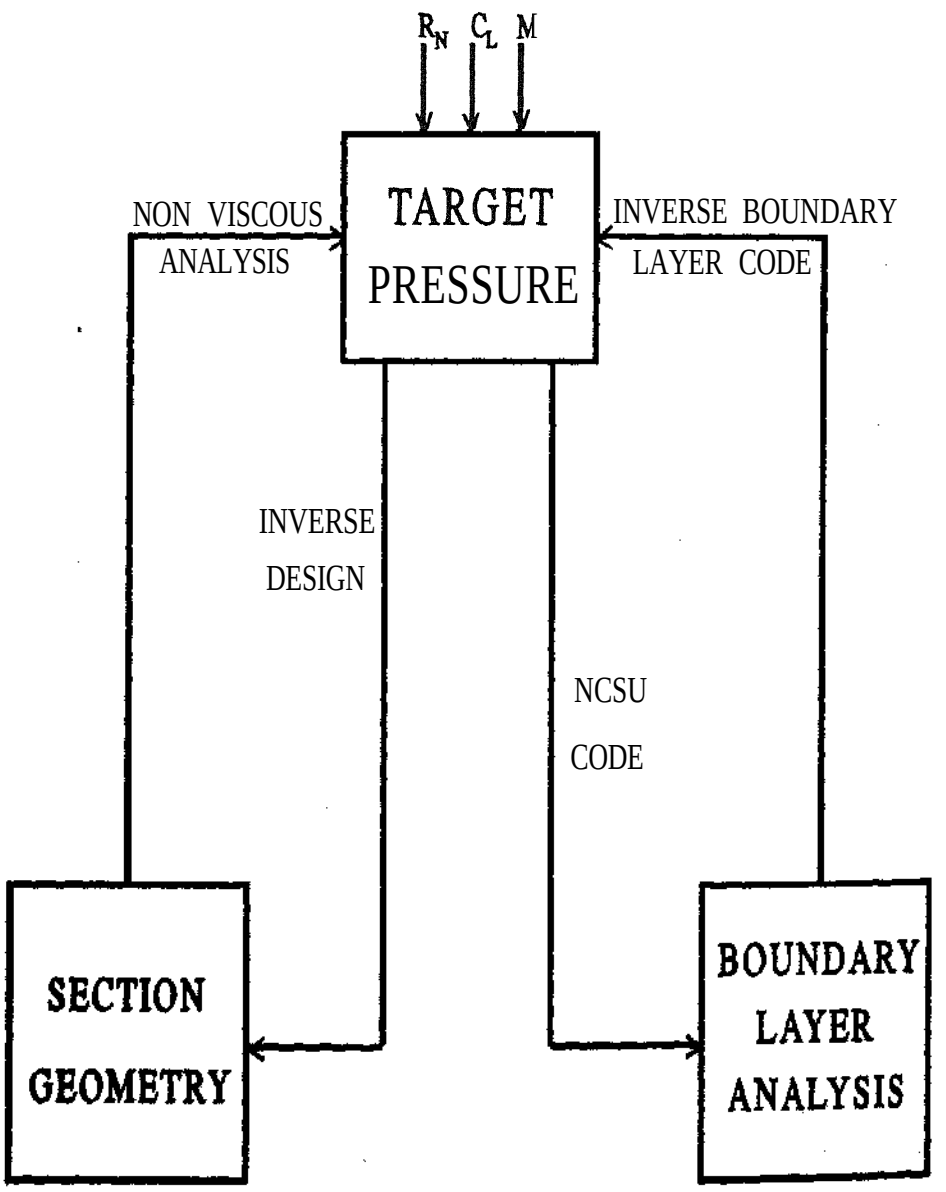

Figure 1. Connection between the boundary-layer development, pressure distribution and section geometry.

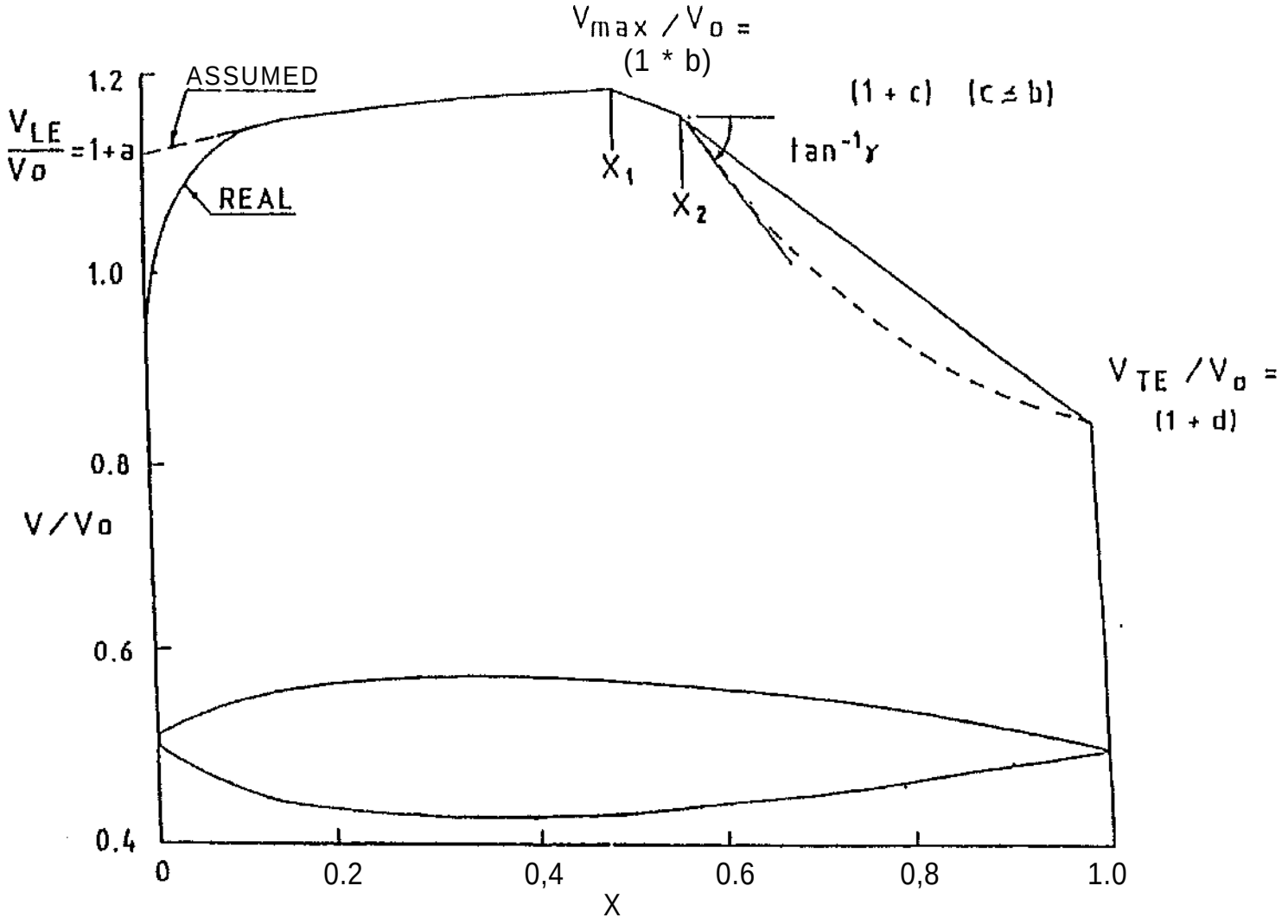

Fig.2 A PLAUSIBLE MODEL FOR NATURAL LAMINAR FLOW AIRFOIL DESIGN

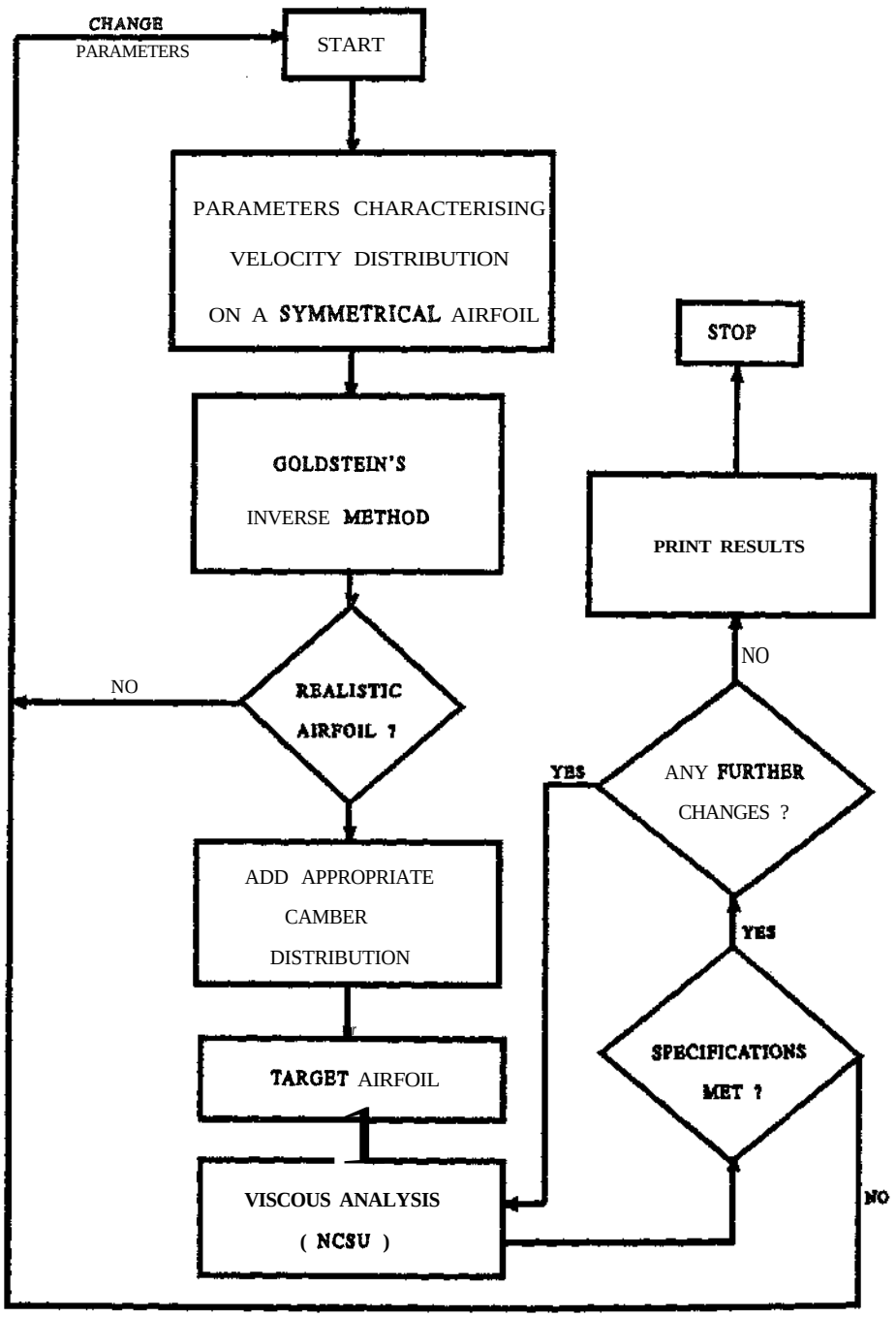

Figure 3. Flow chart for NLF Airfoil design

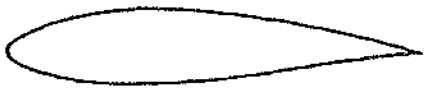

NACA 643 – 418

NACA 643-418

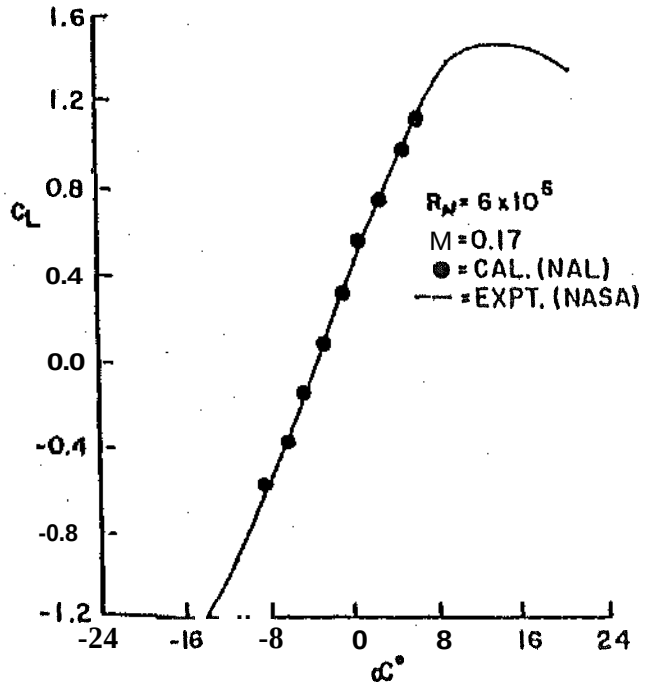

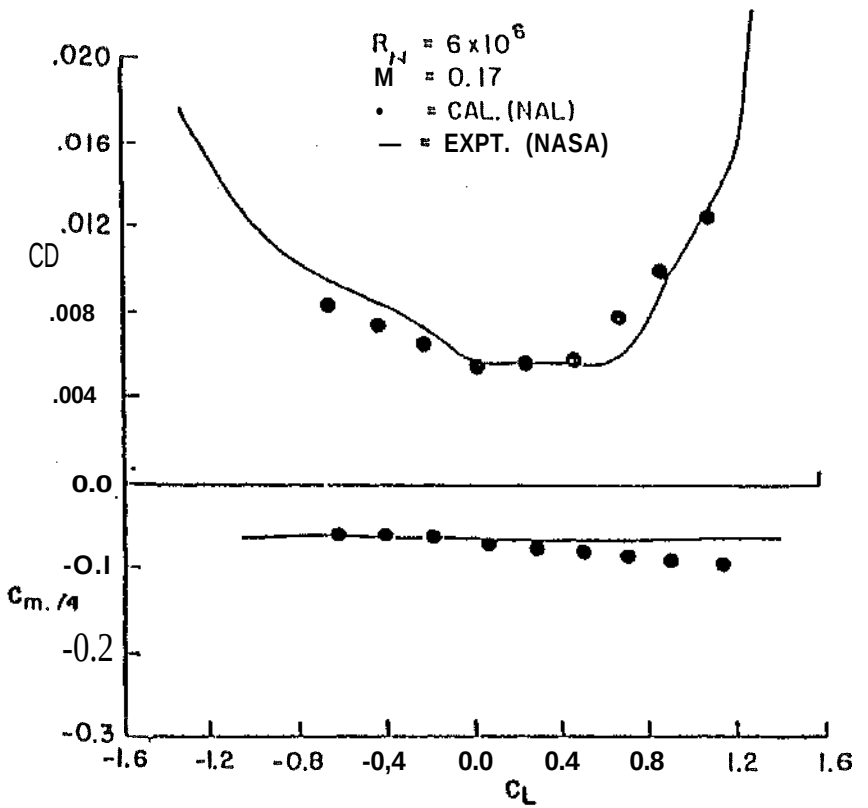

Fig. 4 AERODYNAMIC PERFORMANCE OF NACA 64 – 418 AIRFOIL

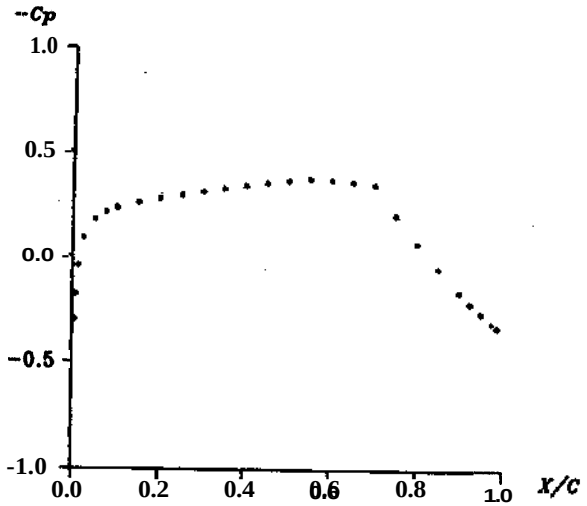

FIG.5 *Cp OF SYMMETRICAL NLF AIRFOIL*

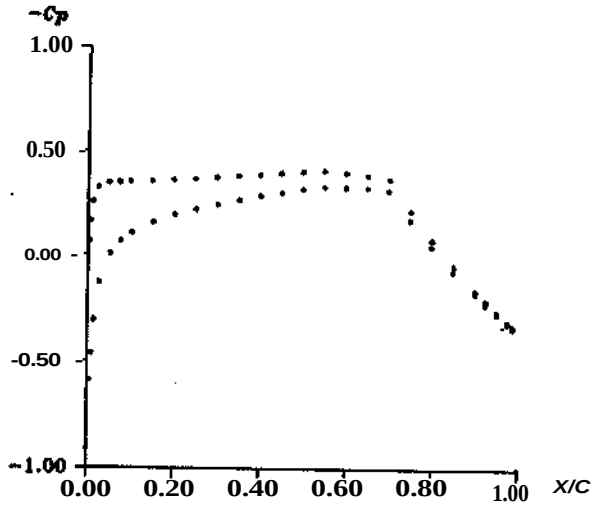

FIG.6 *Cp OF DESIGNED NLF AIRFOIL*

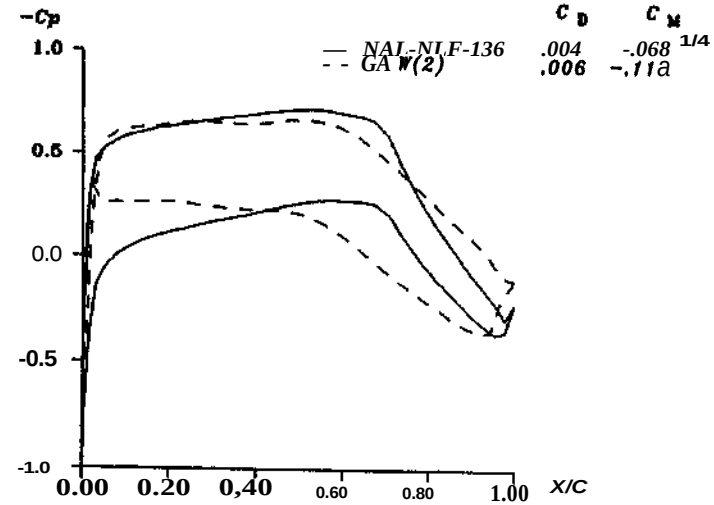

Fig.7 Cp OF NAL-NLF-136 & GAW(2) AIRFOILS AT C_L *=.4* R_N *=10E6 M=.6*

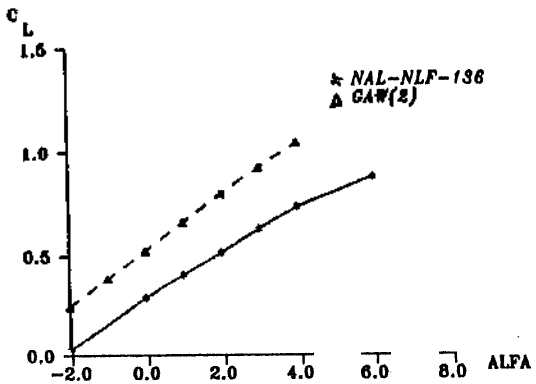

*Fig.8 C_L CURVES OF NAL-NLF-136 * GAW(Z) AIRFOILS AT R_N=10E6 M=.6*

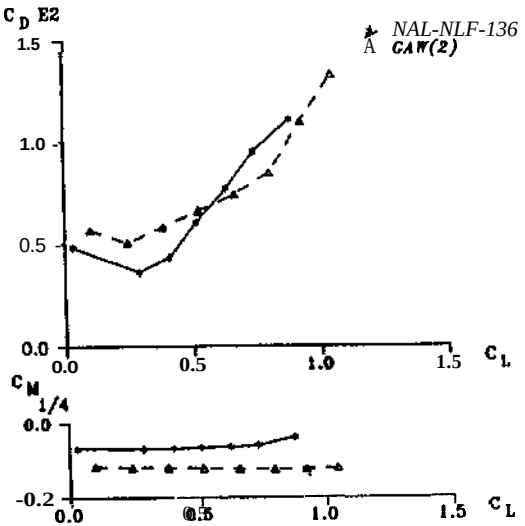

*Fig.9 C_D AND C_M CURVES OF NAL-NLF-136 * GAW(2) AIFOILS AT R_N=10E6 M=.6*

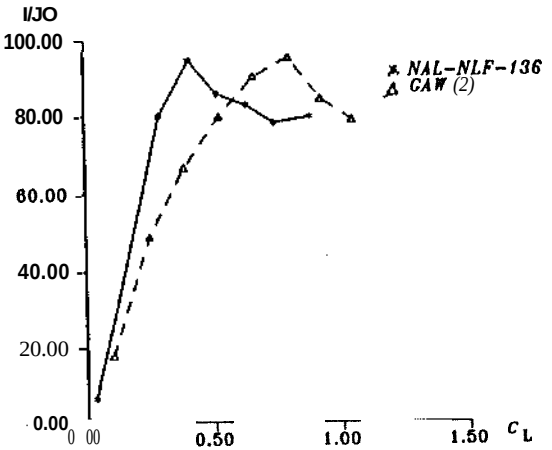

Fig.10 L/D CURVES FOR NAL-NLF-136 A CAW(2) AIRFOILS AT R_N=10E6 M=.6

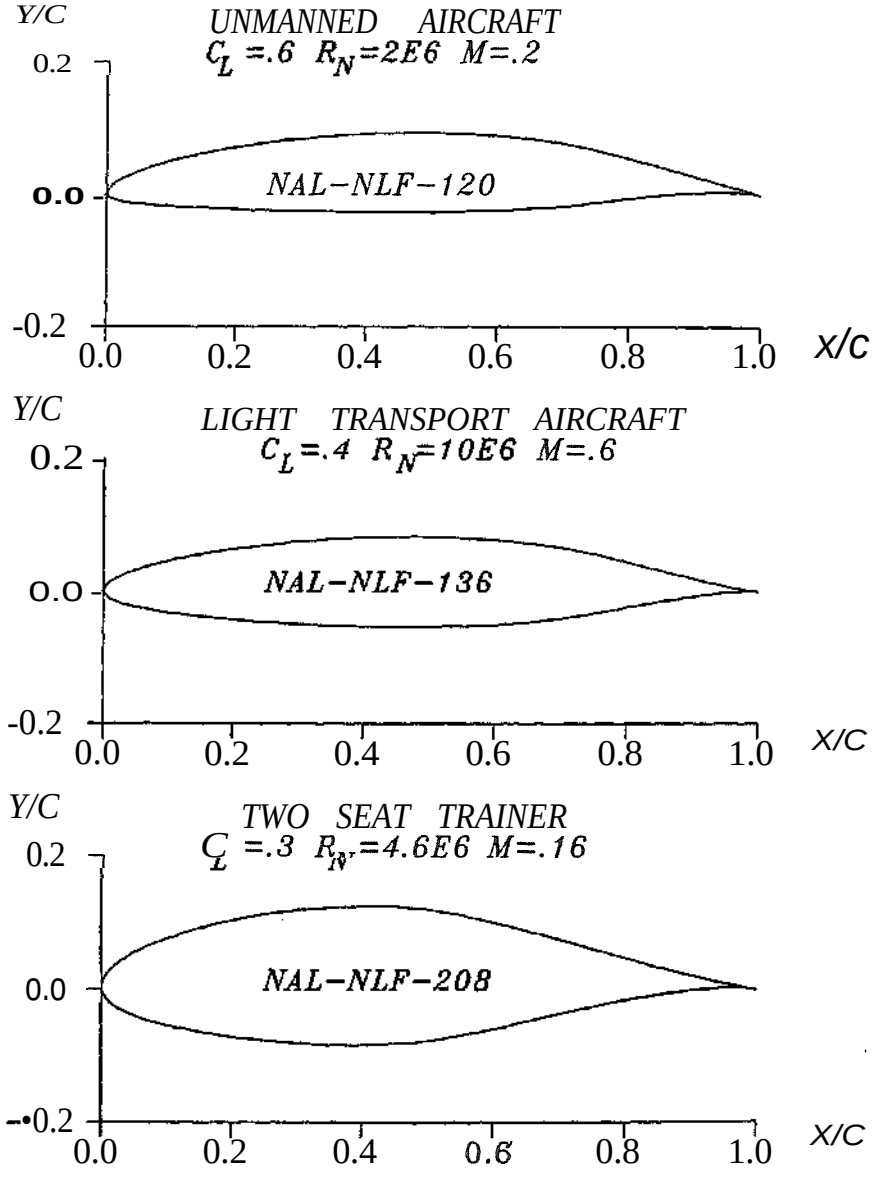

Fig. 11 NAL'S NATURAL LAMINAR FLOW AIRFOILS

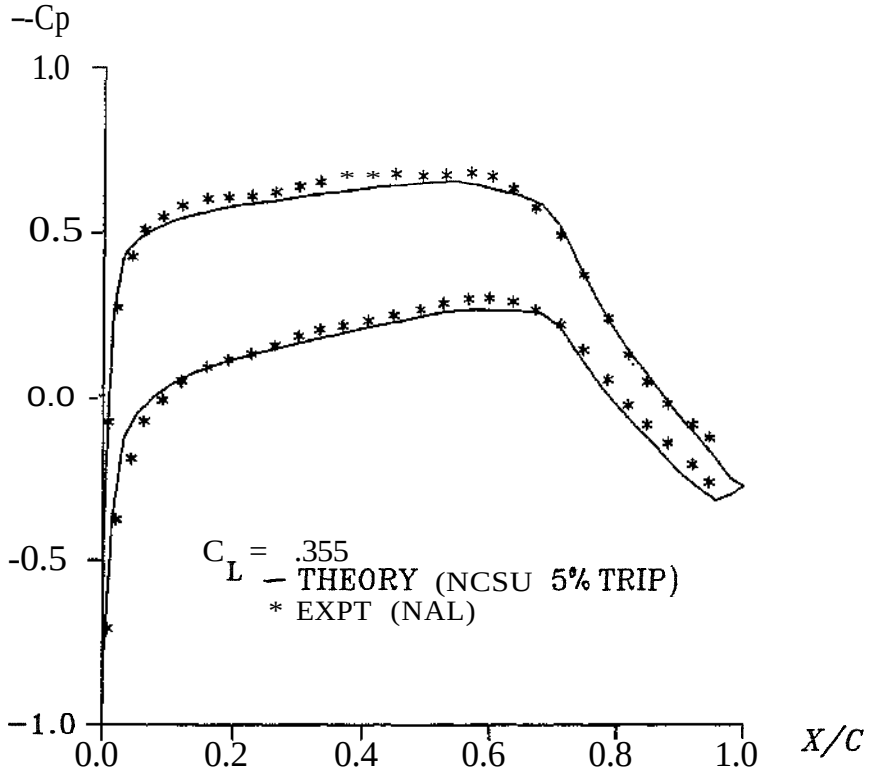

Fig. 12 PERFORMANCE OF NAL–NLF–136 AIRFOIL AT R_N =2.6E6 M=.52